Lubrication Condition Assessment of Planetary Roller Screw under Varying Operating Parameters

Zhichao Dong[1], Yixiang Huang[1], Pengcheng Xia[1], Shidong Zhang[1], and Chengliang Liu[1]

[1] *State Key Laboratory of Mechanical System and Vibration, Shanghai Jiao Tong University, Shanghai 200240, PR China*
mezcdong@sjtu.edu.cn
huang.yixiang@sjtu.edu.cn
xpc19960921@sjtu.edu.cn
alvinzsd@sjtu.edu.cn
chlliu@sjtu.edu.cn

ABSTRACT

The planetary roller screw mechanism (PRSM) is a critical transmission component in electromechanical actuators. Under prolonged operation in harsh service conditions, PRSMs are prone to lubrication deficiencies, which significantly increase the risk of mechanical failure. Consequently, it is essential to develop evaluation techniques for the lubrication condition of PRSMs to enable efficient health management. This study proposes an assessment method for PRSM lubrication status during operation based on a vibration mechanism model. The model integrates the contact characteristics of the threads and operating parameters to characterize the influence of internal lubrication conditions on the system's vibration response. Based on this model, a dimensionless evaluation metric was developed that depends on the amount of lubricant used. Using a dedicated experimental test rig, vibration signals were collected under varying screw rotational speeds, axial loads, and lubricant quantities to validate the method. The experimental results demonstrate the effectiveness of the proposed method in evaluating the lubrication state under varying operating conditions using a small amount of vibration data.

1. INTRODUCTION

The planetary roller screw is a rolling screw transmission mechanism that converts rotational motion into linear motion. By transmitting power through multiple contact surfaces in thread engagement, it offers high load-bearing capacity and exceptional transmission precision (Fu, Liu, Ma, Tong, & Li, 2020). As the core actuator in electromechanical systems, PRSMs are widely employed in aerospace, automotive engineering, marine applications, and intelligent manufacturing (Wu, Ma, Fu, Zhang, & Liu, 2022). The lubrication condition of a PRSM is a critical factor that determines its service life, transmission performance, and overall reliability (Han et al., 2018). In practical engineering applications, factors such as seal aging, lubricant degradation, or insufficient supply often lead to oil-starved conditions. Under such conditions, the lubricant film cannot effectively separate the metal surfaces, resulting in severe interfacial friction, increased temperature, and abnormal vibrations. These effects can degrade motion accuracy and may even cause premature fatigue failure (Miao, Du, Li, Shan, & Chen, 2022). Therefore, early detection of lubrication degradation and timely intervention are essential for effective health management of PRSMs in long-term service.

Vibration sensors have been used in some studies on lubrication assessment due to their high sensitivity and non-intrusive characteristics (Ma, Li, Yang, & Wang, 2025). Currently, deep learning approaches, such as convolutional neural networks (CNNs) and recurrent neural networks (RNNs), enable end-to-end adaptive feature extraction and condition recognition directly from raw vibration signals (Sajjadi, Dinmohammadi, & Shafiee, 2025). However, these approaches require large-scale labeled datasets, resulting in significant time and computational costs (Ferreira & Gonçalves, 2022). In contrast, physics-based methods grounded in lubrication mechanisms demonstrate distinct advantages for rapid condition evaluation. These approaches can accurately quantify the intrinsic relationships among interfacial lubrication state, friction characteristics, and system operating parameters, enabling effective assessment without excessive reliance on monitoring data (Bertolino, De Martin, Fasiello, Mauro, & Sorli, 2022). Nevertheless, few studies have proposed dedicated physical evaluation models that specifically capture the coupled lubrication–vibration mechanisms of PRSMs.

This paper proposes a lubrication condition Assessment method

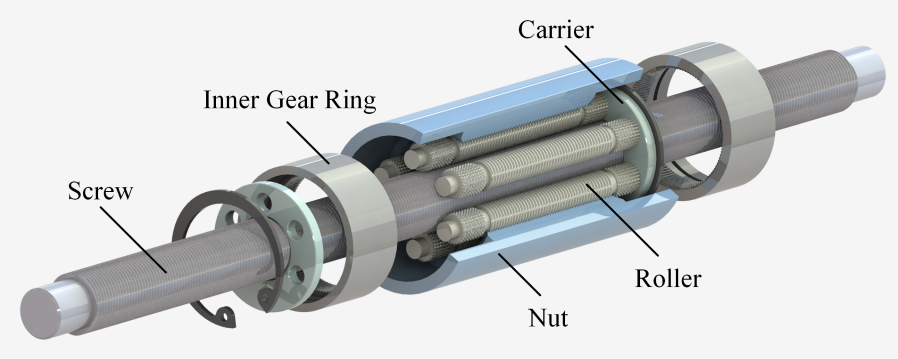

Figure 1. Structural diagram of the planetary roller screw.

for PRSM based on a vibration physics model, which considers the coupled effects of lubricant volume and varying operating conditions. The structure of the paper is as follows: Section 2 develops a dimensionless evaluation metric related to lubricant volume. Furthermore, the mapping relationship between this metric and the ball screw rotational speed, axial load, and vibration amplitude is derived. Section 3 validates the method through experiments conducted under three different lubrication states. Finally, Section 4 summarizes the conclusions of the paper.

2. THE PRINCIPLE OF LUBRICATION CONDITION ASSESSMENT

2.1. PRSM Motion Parameters

A standard planetary roller screw mechanism consists of a screw, a nut, planetary rollers, a carrier, and an internal ring gear, as shown in Figure 1. Each planetary roller is a cylindrical component with external threads that mesh simultaneously with the threads on the screw and the nut, transmitting loads through point contact. The internal ring gear engages with the end gears of the rollers, constraining their motion and ensuring synchronous rotation of all rollers.

In order to model lubrication and vibration, the relative sliding velocity at the thread contact points must first be defined. Let the angular velocity of the screw be denoted by ω_S. Based on the relationship between the mean diameters of the screw thread and the roller thread, the angular velocities of the roller's revolution ω_P and rotation ω_R can be expressed as follows (Velinsky, Chu, & Lasky, 2008):

$$\omega_P = \frac{d_S}{2\left(d_S + d_R\right)}\omega_S \tag{1}$$

$$\omega_R = \frac{d_S\left(d_S + 2d_R\right)}{2d_R\left(d_S + d_R\right)}\omega_S \tag{2}$$

Here, d_S and d_R represent the mean diameters of the screw and the roller threads, respectively. Considering the Hertzian contact deformation theory, the relative sliding velocity v_{SR}^i for the i-th thread engagement pair between the screw and the roller can be expressed as follows:

$$v_{SR}^i = v_R^i - v_S^i \tag{3}$$

Here, v_S^i and v_R^i represent the velocities at the i-th thread engagement pair, on the screw side and the roller side, respectively, and can be expressed as (Xie et al., 2019):

$$v_S^i = \left(\frac{d_S}{2} - \delta_{SR}^i \cos\beta\right)\omega_S \cos\alpha_S \tag{4}$$

$$v_R^i = \left[\omega_R\left(-d_R - 2\delta_{SR}^i\cos\beta\right) - \frac{d_S\omega_S\tan^2\alpha_S}{2}\right]\cos\alpha_S \tag{5}$$

Here, β is the flank angle of the thread, α_S is the lead angle of the screw, and δ_{SR}^i is the contact deformation at the i-th thread engagement point between the screw and the roller. Therefore, Eq. (3) can be expressed as:

$$\begin{aligned} v_{SR}^i = &\left[(\omega_S - 2\omega_R)\delta_{SR}^i\cos\beta - d_S\omega_S\left(1+\tan^2\alpha_S\right)/2\right. \\ &\left. - d_R\omega_R\right]\cos\alpha_S \end{aligned} \tag{6}$$

Simplifying the equation, we obtain:

$$v_{SR}^i = k_v^i\omega_S \tag{7}$$

where k_v^i is a parameter related to the geometry, material, and load distribution.

2.2. Lubrication Model

The Stribeck curve is commonly used to describe the nonlinear variation of lubrication in screws. This curve divides the lubrication state into boundary lubrication, mixed lubrication,

and fluid lubrication, as shown in Figure 2. The control of the lubrication state depends on the viscosity η of the lubricating oil, the relative sliding velocity v at the contact points and the contact surface pressure p (Zhang & Zhou, 2022). At low speeds, high loads, and insufficient lubrication supply, the friction pair is prone to transition from fluid lubrication to mixed lubrication and even to boundary lubrication. During this process, the coefficient of friction exhibits complex nonlinear evolution characteristics. This chapter simplifies the lubrication evaluation model by introducing a dimensionless lubrication supply factor.

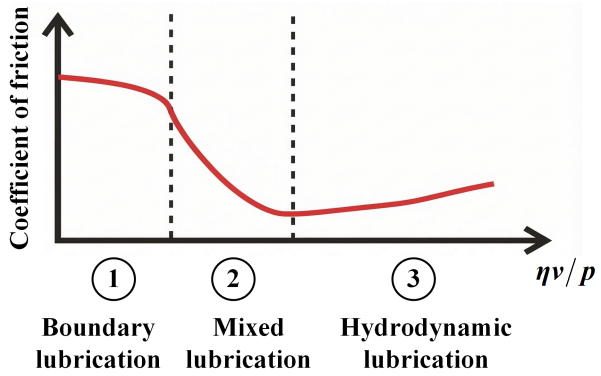

Figure 2. Stribeck curve.

When sufficient lubricating oil is supplied, fluid lubrication with complete separation of the contact surfaces can be achieved by optimizing the screw rotational speed and load. Suppose that the initial lubrication state of the screw is in this condition. According to the Hamrock–Dowson equation (Hamrock & Dowson, 1977), the dimensionless minimum film thickness H_{min} of a point-contact friction pair is given by:

$$H_{\min} = 3.63U^{0.68}G^{0.49}W^{-0.073}\left(1 - e^{-0.68k}\right) \tag{8}$$

where U, G, and W are the dimensionless velocity, material, and load parameters, respectively, and k is the contact ellipticity factor. The increase in speed can significantly thicken the oil film through the hydrodynamic wedge effect, while an increase in load will cause the oil film to be slightly thin. For a given planetary roller screw, under fully lubricated conditions, the theoretical minimum oil film thickness in the i-th thread engagement zone between the screw and the roller can be expressed as:

$$H^i_{min} = C_h \left(v^i_{SR}\right)^{0.68} \left(F^i_{SR}\right)^{-0.073} \tag{9}$$

where C_h is the system constant that combines material properties and geometric parameters, and F^i_{SR} is the contact force between the thread teeth. As the screw continues to operate, the lubricating oil experiences centrifugal loss. When the effective oil supply in the contact zone decreases to the level that triggers lubrication starvation, the actual oil film thickness becomes smaller than the theoretical calculated thickness. A dimensionless lubrication supply factor θ_{Oil}, which characterizes the adequacy of the oil supply, is introduced:

$$H^i_{actual} = \theta_{Oil} H^i_{min} \tag{10}$$

Assuming that when lubrication is sufficient, $\theta_{Oil} = 1$, and when lubrication starvation occurs, $\theta_{Oil} < 1$. The film thickness ratio λ is a key parameter in tribology for characterizing the lubrication state, defined as the ratio of the minimum oil film thickness to the root mean square of the surface's combined roughness:

$$\lambda^i = \frac{H^i_{actual}}{\sigma} \tag{11}$$

If the effect of surface wear is neglected, σ^i can be considered a constant. Based on the micro-roughness peak contact theory, the probability of roughness peak contact and the high-frequency vibrational energy it excites decay exponentially with the film thickness ratio (Mohd Yusof & Ripin, 2014). Therefore, the nonlinear excitation factor for system vibration due to the lubricating oil quantity can be modeled as:

$$\Phi^i_{Oil} = \exp(-\lambda^i) = \exp\left[-\theta_{Oil} C^i_\lambda \left(v^i_{SR}\right)^{0.68} \left(F^i_{SR}\right)^{-0.073}\right] \tag{12}$$

where C^i_λ is a constant that represents the contact characteristics of the thread surface.

2.3. Vibration-Based Lubrication Evaluation Metric

Based on the lumped parameter method, assume the PRSM system is a simplified single-degree-of-freedom vibration system. According to Newton's second law, the system's motion differential equation can be expressed as:

$$m_{eq}\ddot{x} + c_{eq}\dot{x} + k_{eq}x = F_{ex}(t) \tag{13}$$

Where m_{eq} is the equivalent mass of motion, c_{eq} is the system's equivalent damping coefficient, k_{eq} is the equivalent stiffness, and $F_{ex}(t)$ is the time-varying external excitation force. x, $\dot{x}$ and $\ddot{x}$ represent the vibration displacement, velocity, and acceleration, respectively. In the steady-state operation phase, far from the resonance zone, the amplitude X_0 of the system's vibration response displacement can be approximated as:

$$X_0 \approx \frac{F_0}{K_0} \tag{14}$$

Where F_0 and K_0 represent the amplitudes of the external excitation force and system stiffness, respectively. Acceleration is the second derivative of displacement. At the dominant frequency ω, the relationship between the acceleration amplitude A_0 and X_0 is given by $A_0 \approx \omega^2 X_0$. The dominant frequency is usually proportional to the lead screw angular velocity, therefore:

$$A_0 \propto \omega_S^2 \frac{F_0}{K_0} \tag{15}$$

According to Hertz contact theory, when two helical surfaces bear a normal load, local elastic deformation occurs at the contact points, forming a contact ellipse. By integrating the load distribution over this contact area, the elastic deformation of the two contacting bodies can be calculated. Therefore, the formula for the normal contact deformation at the thread-tooth contact points on the screw–roller side or nut–roller side can be expressed as:

$$\delta = \frac{2K(e)}{\pi m} \cdot \left(\frac{3F_n E'}{2\sum \rho} \right)^{\frac{2}{3}} \cdot \frac{\sum \rho}{2} \tag{16}$$

Here, E' is the equivalent elastic modulus, $K(e)$ represents the complete elliptic integral of the first kind, e is the eccentricity, m is a coefficient related to the curvature difference function, $\sum \rho$ is the sum of the principal curvatures of the contacting bodies, and F_n is the normal contact force. The normal contact stiffness K_n can be expressed as:

$$K_n = \frac{dF_n}{d\delta} = k_\delta F_n^{1/3} \tag{17}$$

where k_δ is a constant related to the geometry and material properties of the two contacting surfaces. This indicates that, in the PRSM dynamic system, the stiffness of the thread contact region increases with the load, exhibiting a stiffening effect.

In addition to affecting the oil film thickness and contact stiffness, the load also changes the interface friction and relative sliding velocity. Therefore, it is a complex external excitation source. For the convenience of theoretical derivation and model simplification, this paper defines the excitation term derived from the load acting on the interface friction and sliding as the load excitation factor:

$$\Phi_F = \exp\left(C_F F_a\right) \tag{18}$$

where, C_F is the load influence coefficient determined by the structure and oil properties, and F_a is the axial load. It is assumed that the load is uniformly distributed between multiple rollers and between the threads of a single roller in the PRSM, meaning the normal contact force on each thread is the same. Therefore, Eq. (12) and (17) can be expressed as:

$$\Phi_{Oil} = \exp\left[-\theta_{Oil} C_\lambda \omega_S^{0.68} F_a^{-0.073}\right] \tag{19}$$

$$K_0 \propto F_a^{1/3} \tag{20}$$

In addition, the amplitude of the external excitation force can be expressed as the product of the lubricant excitation factor and the load excitation factor:

$$F_0 \propto \Phi_{Oil} \Phi_F \tag{21}$$

According to Eq. (15), (20) and (21), the acceleration amplitude A_0 can be expressed as:

$$A_0 = C_{sys} \omega_S^2 F_a^{-1/3} \exp\left[C_F F_a - \theta_{Oil} C_\lambda \omega_S^{0.68} F_a^{-0.073}\right] \tag{22}$$

Therefore, by considering the effects of the lead screw rotational speed, lubricant amount, and axial load on the vibration signal, the lubrication evaluation metric based on the vibration signal can be constructed as:

$$\theta_{Oil} = \frac{C_F F_a - \ln\left(C_{sys}^{-1} A_0 \omega_S^{-2} F_a^{1/3}\right)}{C_\lambda \omega_S^{0.68} F_a^{-0.073}} \tag{23}$$

where C_{sys} is the system's inherent constant.

3. EXPERIMENTAL VALIDATION

3.1. Experimental Setup

To verify the accuracy of the proposed lubrication evaluation metric, a PRSM test rig was built as shown in Figure 3. The test rig was used to collect vibration signals under different lead screw rotational speeds and axial loads. The nut was fixed beneath the workbench to constrain it to axial linear motion along the lead screw only. The lead screw rotational speed was measured using an angular encoder at the motor end. An electromagnetic loading device applied adjustable axial loads to the workbench. A force sensor with an accuracy of 0.03% was installed between the workbench and the loading device to measure the output force of the PRSM. Additionally, a piezoelectric accelerometer with a sensitivity of 100 mV/g was arranged on the nut end surface to acquire the axial vibration response of the PRSM. All vibration signals were synchronously collected by an NI data acquisition system at a sampling frequency of 4 kHz.

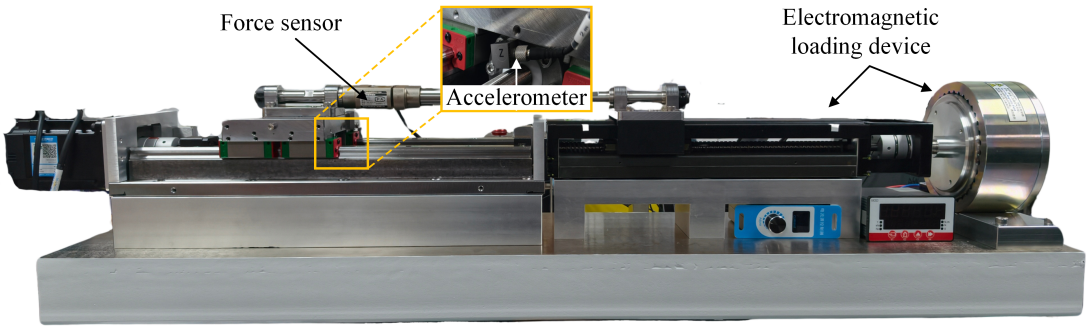

Figure 3. PRSM test rig.

The lubrication evaluation metric proposed in this study is shown in Eq. (23), which includes three parameters C_{sys}, C_F and C_λ to be identified. In actual operation, the vibration characteristics vary when the nut is at different axial positions along the lead screw. Therefore, these parameters usually exhibit spatiotemporal variability, making high-precision real-time dynamic identification challenging. To improve identification efficiency, this study approximates these three parameters as constants. The specific experimental scheme is as follows:

1. The lead screw rotational speeds were set to 100 r/min, 150 r/min, and 200 r/min, and the axial loads were set to 100 N and 200 N, forming a total of six cross-operating conditions.
2. A stepwise lubrication method was adopted, in which lubricant was injected into the nut through the oil port in three steps, with 2 mL per injection. After each lubrication step, all six operating conditions were immediately traversed. Based on the collected vibration data, the three parameters to be identified were fitted using the least squares method.
3. During testing, the nut was fed in a single direction away from the motor side, with a total travel of 180 mm. After excluding the acceleration and deceleration phases, the effective travel was 170 mm. Positioning was realized using the motor's absolute encoder to ensure that the start and end positions of each run were consistent.

3.2. Results

Figure 4 shows the raw axial vibration signals under different operating conditions and amounts of lubricating oil. It can be observed that as the nut feeds away from the motor side, the amplitude of the vibration signal slightly decreases. This is attributed to the position-dependent stiffness of the lead screw shaft. The root mean square (RMS) of the raw vibration signals within the effective travel was used to characterize the overall amplitude A_0 of the vibration acceleration, with the statistical results shown in Figure 5(a). The experimental results indicate that the RMS is most affected by rotational speed, which is attributed to the role of ω_S^2 in Equation (22). When the speed increases from 100 r/min to 200 r/min, the RMS significantly increases. In addition, when the load increases from 100 N to 200 N, the vibration amplitude slightly decreases, since $F_a^{-1/3}$ dominates under light load rather than $exp(C_F F_a)$. It is noteworthy that under the same operating condition, as lubricating oil is incrementally injected, the RMS value shows a decreasing trend, confirming the correlation between the vibration response amplitude and the interface lubrication state.

The vibration data after the third lubrication injection were used as the reference for parameter identification, assuming that the lead screw was in a fully fluid-lubricated state with $\theta_{Oil} = 1$. Based on the RMS vibration data under six operating conditions in this state, the values of C_{sys}, C_F and C_λ were obtained through least squares fitting. Then, the measured vibration data from the first two lubrication stages, along with the corresponding operating condition parameters, were input into the calibrated model to enable a quantitative evaluation of the PRSM at different lubrication levels. The results are presented in Figure 5(b), where the mean values of θ_{Oil} after the first and second lubrication injections are 0.72 and 0.83, respectively. Under the same lubrication amount, the lubrication evaluation indices corresponding to different operating conditions remain largely at the same level, validating the effectiveness of the proposed method. This metric decreases as the amount of lubricant decreases, reflecting the system's transition from a fluid-lubricated state to a starved-lubrication condition.

4. CONCLUSION

This paper proposes an evaluation method for the lubrication state of PRSM based on a vibration mechanism model. The method derives the kinematic relationship between the relative sliding velocity and lead screw rotational speed based on Hertzian contact theory, accounting for the influence of thread engagement. Then, by incorporating the minimum oil film

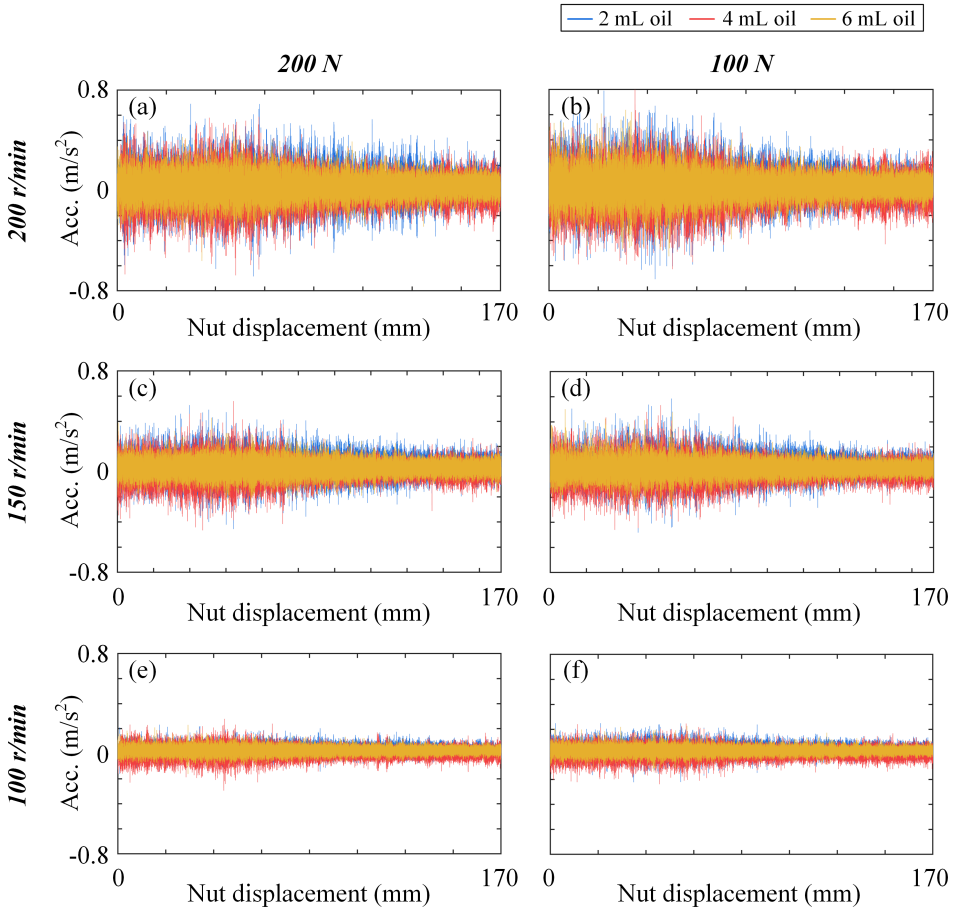

Figure 4. Raw axial vibration signals under different operating conditions and lubricant levels.

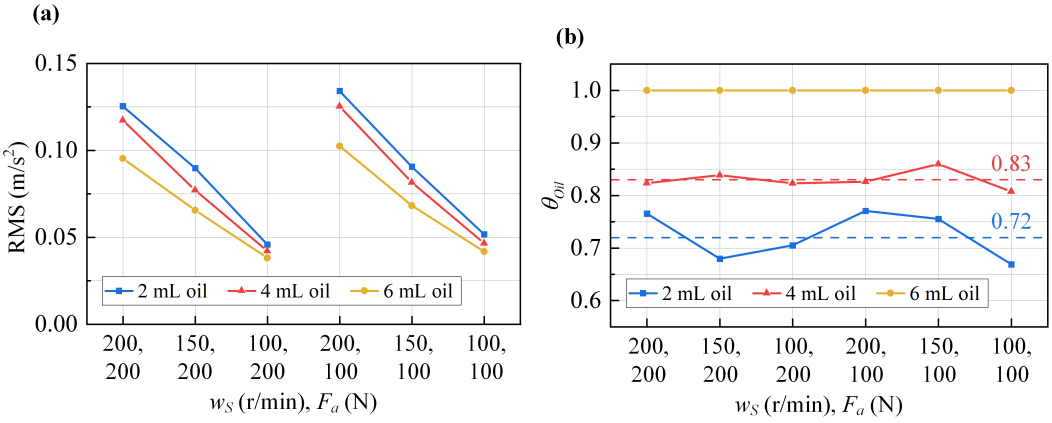

Figure 5. RMS and θ_{Oil} of vibration signals under different operating conditions and lubricant levels

thickness model, a dimensionless lubrication supply factor is introduced to assess the lubrication oil quantity. Building on this, a simplified dynamic model is used to derive the mapping relationship between the evaluation metric and lead screw speed, axial load, and vibration response. Using a dedicated PRSM test rig, vibration tests were conducted across six operating conditions and three lubrication oil levels. The results show that the measured vibration amplitudes follow the same trend as predicted by the theoretical mechanism model. Furthermore, the proposed evaluation metric exhibits a significant decreasing trend as the lubrication oil quantity decreases. This validates the effectiveness of the proposed

method in evaluating the lubrication state under varying operating conditions using a small amount of vibration data.

ACKNOWLEDGMENT

This research was supported by the National Natural Science Foundation of China (No. 52405122) and the China Postdoctoral Science Foundation (No. 2025M771378).

REFERENCES

Bertolino, A. C., De Martin, A., Fasiello, F., Mauro, S., & Sorli, M. (2022). A simulation study on the effect of lubricant ageing on ball screws behaviour. In *2022 international conference on electrical, computer, communications and mechatronics engineering (iceccme)* (pp. 1–7).

Ferreira, C., & Gonçalves, G. (2022). Remaining useful life prediction and challenges: A literature review on the use of machine learning methods. *Journal of manufacturing systems*, *63*, 550–562.

Fu, X., Liu, G., Ma, S., Tong, R., & Li, X. (2020). An efficient method for the dynamic analysis of planetary roller screw mechanism. *Mechanism and Machine Theory*, *150*, 103851.

Hamrock, B. J., & Dowson, D. (1977). Isothermal elastohydrodynamic lubrication of point contacts: part iii—fully flooded results. *ASME. J. of Lubrication Tech*, *99*(2), 264-275.

Han, C.-F., He, H.-Q., Wei, C.-C., Horng, J.-H., Chiu, Y.-L., Hwang, Y.-C., & Lin, J.-F. (2018). Techniques developed for fault diagnosis of long-range running ball screw drive machine to evaluate lubrication condition. *Measurement*, *126*, 274–288.

Ma, L., Li, Z., Yang, S., & Wang, J. (2025). A review on vibration sensor: Key parameters, fundamental principles, and recent progress on industrial monitoring applications. *Vibration*, *8*(4), 56.

Miao, J., Du, X., Li, C., Shan, X., & Chen, B. (2022). Lubrication and wear analysis of planetary roller screw mechanism with threaded surface roughness in thermal elastohydrodynamic lubrication. *Tribology Transactions*, *65*(6), 1069–1087.

Mohd Yusof, N. F., & Ripin, Z. M. (2014). Analysis of surface parameters and vibration of roller bearing. *Tribology Transactions*, *57*(4), 715–729.

Sajjadi, P., Dinmohammadi, F., & Shafiee, M. (2025). Machine learning in prognostics and system health management of cyber-physical systems: A review. *IEEE Access*.

Velinsky, S. A., Chu, B., & Lasky, T. A. (2008, 12). Kinematics and efficiency analysis of the planetary roller screw mechanism. *ASME. J. Mech. Des*, *131*(1), 011016.

Wu, L., Ma, S., Fu, X., Zhang, J., & Liu, G. (2022). A review of planetary roller screw mechanism for development and new trends. *Proceedings of the Institution of Mechanical Engineers, Part C: Journal of Mechanical Engineering Science*, *236*(21), 10822–10840.

Xie, Z., Xue, Q., Wu, J., Gu, L., Wang, L., & Song, B. (2019). Mixed-lubrication analysis of planetary roller screw. *Tribology International*, *140*, 105883.

Zhang, L.-C., & Zhou, C.-G. (2022). Experimental study on the coefficient of friction of the ball screw. *ASME. J. Tribol*, *144*(3), 031601.